Atmos. Chem. Phys. Discuss., https://doi.org/10.5194/acp-2017-718
Manuscript under review for journal Atmos. Chem. Phys.
Discussion started: 14 August 2017

Atmospheric Chemistry and Physics Discussions

Temporally-Delineated Sources of Major Chemical Species in High Arctic Snow

Katrina M. Macdonald[1], Sangeeta Sharma[2], Desiree Toom[2], Alina Chivulescu[2], Andrew Platt[2], Mike Elsasser[2], Lin Huang[2], Richard Leaitch[2], Nathan Chellman[3], Joseph R. McConnell[3], Heiko Bozem[4], Daniel Kunkel[4], Ying Duan Lei[1], Cheol-Heon Jeong[1], Jonathan P. D. Abbatt[5], Greg J. Evans[1]

[1]Department of Chemical Engineering and Applied Chemistry, University of Toronto, M5S 3E5, Canada
[2]Climate Research Division, Environment and Climate Change Canada, Toronto, M3H 5T4, Canada
[3] Desert Research Institute, Reno, 89512, Unites States of America
[4] Institute for Atmospheric Physics, Johannes Gutenberg University Mainz, Becher Weg, 21 55128, Germany
[5] Department of Chemistry, University of Toronto, M5S 3H6, Canada

Correspondence to: Greg J. Evans (greg.evans@utoronto.ca)

Abstract. Long-range transport of aerosol from lower latitudes to the high Arctic may be a significant contributor to climate forcing in the Arctic. To identify the sources of key contaminants entering the Canadian high Arctic an intensive campaign of snow sampling was completed at Alert, Nunavut, from September 2014 to June 2015. Fresh snow samples collected every few days were analysed for black carbon, major ions, and metals, and this rich data provided an opportunity for a temporally-refined source apportionment of snow composition via Positive Matrix Factorization in conjunction with FLEXPART potential emission sensitivity analysis. Seven source factors were identified: sea salt, regional dust, Eurasian fossil fuel combustion, mixed carboxylic acid sources, nitrate processing, Eurasian industrial activities, and regional volcanic and marine biogenic activity. The majority (73%) of the black carbon in snow, a light-absorbing compound critical to the Arctic radiative balance, was found to be the product of fossil fuel burning with limited biomass burning influence.

1 Introduction and Background

Observations of Arctic climate have shown pronounced changes over recent years, including a rapid rise in surface temperature and the loss of sea ice and snow cover, with adverse local and global consequences (AMAP, 2011; Hartmann et al., 2013). Such changes in Arctic climate have been tied to contaminants within the Arctic atmosphere and snow, especially light absorbing compounds such as black carbon (BC) which can warm the surface and atmosphere (Clarke and Noone, 1985; Hansen and Nazarenko, 2004; Bond et al., 2013; Jiao et al., 2014). Furthermore, studies have found the long-range transport of lower-latitude anthropogenic and natural emissions to be a significant and substantial contributor to the Arctic aerosol burden (Stohl, 2006; Law and Stohl, 2007; AMAP, 2015). Thus, understanding the sources of these pollutants is a critical step in the development of control and mitigation strategies to protect the vulnerable Arctic environment.

The lower troposphere of the Arctic is separated from the upper and southerly atmosphere by a transport barrier known as the "Arctic front" or "Arctic dome". This dome is formed by surfaces of constant potential temperature, which inhibit the transport

of southerly air masses into the lower Arctic troposphere, instead forcing northward-travelling air masses to rise over the dome. The size and location of the Arctic front is a complex system driven by global atmospheric conditions, with significant variation by season. Over the summer, the Arctic front is typically northward of 70 °N; however, during the winter the Arctic front extends farther south, as far as 40 °N (Stohl, 2006; Law and Stohl, 2007; AMAP, 2015). The Arctic front is also zonally asymmetric, typically extending much farther south over Eurasia during the winter. Thus, the Arctic atmosphere is more vulnerable to transport from southerly sources in the winter than the summer, especially Eurasian sources. Particles entering the Arctic atmosphere can be removed only by atmospheric transport or deposition, and the deposition processes are much slower in the winter than in the summer; thus Arctic snow is a critical reservoir within the Arctic system. Given the seasonal variability in Arctic aerosol inputs and outputs, a period of enhanced accumulation is typically experienced during the Arctic winter and early spring termed "Arctic Haze". The haze is primarily composed of sulphate (SO_4^{2-}) and organic particulate matter with varying levels of ammonium (NH_4^+), nitrate (NO_3^-), mineral dust, and BC (AMAP, 2006; Quinn et al., 2007). Interest in Arctic aerosol increased after the first observations of Arctic Haze in the 1950's (AMAP, 2006), and intensive routine monitoring of the Arctic atmosphere dates back to the late 1970's, particularly monitoring of BC and SO_4^{2-} (Barrie, Hoff, and Daggupaty, 1981). However, direct measurements of pollutants in Arctic snow have been less common, particularly sampling campaigns of fresh snow which are less prone to the ambiguities introduced by snowpack collection. The relative abundance of Arctic aerosol data has facilitated extensive research on particulate sources (e.g., Sirois and Barrie, 1999; Stohl et al., 2013; Nguyen et al., 2013; Yttri et al., 2014). Fewer studies have identified the sources of snow impurities, which represent the deposited and surface albedo-influencing portion of the aerosol, and often these studies are reliant on modelled snow concentrations (e.g., Skeie et al., 2011; Wang et al., 2011) rather than measurements (e.g., Hegg et al., 2009; Hegg et al., 2010). Also, great variability has been seen across existing snow apportionment studies. For example, previous studies show significant disagreement in the apportionment of BC during the Arctic winter, ranging from approximately 10% to over 90% attributed to biomass burning (e.g., Wang et al., 2011 and e.g., Hegg et al., 2009, respectively). To the best of the authors' knowledge, no quantitative source apportionment has previously been conducted using temporally-refined fresh Arctic snow samples. Given the critical consequences arising from the deposition of BC and other impurities in snow, source apportionment specifically of these deposited chemical species is an important step towards understanding the Arctic environment. In this context, this paper analyses the sources of chemical components in freshly-fallen snow samples collected over a complete fall-winter-spring at a high Arctic location (Alert, Nunavut), using a combination of Positive Matrix Factorization diagnostics and Lagrangian dispersion modelling.

2 Methodology

2.1 Snow Sample Collection and Analysis

Sample collection and analysis was completed as per Macdonald et al. (2017). Briefly, fresh snow samples were collected at Alert, Nunavut (82°30' N, 62°20' W), from September 14th, 2014 to June 1st, 2015 from two snow tables located in an open-

Atmos. Chem. Phys. Discuss., https://doi.org/10.5194/acp-2017-718
Manuscript under review for journal Atmos. Chem. Phys.
Discussion started: 14 August 2017

Atmospheric Chemistry and Physics Discussions

air minimal traffic site, about 1 km SSW of the Alert base camp. Replicate samples were collected after each snowfall, weather permitting, to a total of 59 sets of samples ranging from 1 to 19 days between samples with an average of 4 days. The use of a snow table allowed the deposition area associated with each sample to be recorded and used in the conversion of measured concentration to flux, which provided a considerable advantage over previous snow sampling campaigns.

Snow samples were analysed for BC via single particle soot photometry (SP2), major ions via ion chromatography (IC) and pH analyzer, and soluble and insoluble metals via inductively coupled plasma mass spectrometry (ICP-MS) as described in Macdonald et al. (2017). Stringent quality assurances were followed throughout snow collection and analysis. The uncertainty of each measurement was estimated based on analysis detection limits and reproducibility as follows (Reff et al., 2007; Norris et al., 2014):

$$u_{ij} = \sqrt{\left(EF_j\ x_{ij}\right)^2 + \left(\tfrac{1}{2}\ MDL_j\right)^2} \quad ,if\ x_{ij} \geq MDL_j \tag{1}$$

$$u_{ij} = \tfrac{5}{6}\ MDL_j \quad ,if\ x_{ij} < MDL_j$$

$$u_{ij} = 4\ \bar{X}_j \quad ,if\ x_{ij}\ is\ missing$$

where x_{ij} is the i^{th} measured value of analyte j, u_{ij} is the uncertainty associated with this measurement, EF_j is the error fraction for this analyte, $\bar{X}_j$ is the median measurement for this analyte, and MDL_j is the method detection limit for this analyte.

The error fraction of each analyte was calculated as double the standard error of replicate measurements for each analysis, with a minimum of 10% imposed (Macdonald et al., 2017 as per Hegg et al., 2010). The method detection limit of each analyte was calculated as three standard deviations of analyzed blank samples. The uncertainty for any samples with known preparation concerns was doubled (e.g., partial sample melt in transit or poor mass closure over preparation); however, less than 7% of samples were noted as having potential preparation concerns.

The signal-to-noise (S/N) of each analyte was also calculated to indicate the strength of each measurement. Given the enhanced uncertainty of below MDL and missing values, these data points were excluded so as to not under-exaggerate the S/N (Norris et al., 2014). A S/N over 2 was considered to be strong, while a S/N from 0.2 to 2 was considered weak (Paatero and Hopke, 2003).

$$S/_{N_j} = \tfrac{1}{n} \sum_{i=1}^{n} d_{ij} \quad ; \tag{2}$$

$$d_{ij} = \tfrac{x_{ij} - u_{ij}}{u_{ij}} \quad ,if\ x_{ij} > u_{ij}$$

$$d_{ij} = 0 \quad ,if\ x_{ij} < u_{ij}$$

where S/N_j is the signal-to-noise of analyte j, n is the total number of samples, and d_{ij} is a measure of the difference between the measured value and its uncertainty for the i^{th} measurement of this analyte (all other variables are defined as in Eq. 1).

To complement snow measurements, simultaneous meteorological and atmospheric aerosol measurements throughout the campaign were considered, as provided by Environment and Climate Change Canada (ECCC). Local meteorological conditions were monitored by the Alert ECCC stations (Climate IDs 2400306, 2400305, and 2400302) (retrieved Nov. 2015

from climate.weather.gc.ca). Atmospheric composition was monitored at the Alert base camp: BC via hourly SP2 and major ions via IC of 6 to 8-day high-volume filters of total suspended particles (Hi-Vol). All the data are presented in our earlier publication (Macdonald et al., 2017).

2.4 Computational Analyses

Two approaches to source identification were used. Source type was explored via measurement apportionment to identify the source composition and seasonal contribution. Source location was explored via backward particle dispersion modelling.

2.4.1 Source Apportionment

Positive matrix factorization (PMF) is a numerical technique for describing speciated data as factors with associated compositional and temporal profiles. Unlike many other source apportionment methods, PMF offers the distinct advantages of enforced positive factor solutions and weighting of the solution by user-defined uncertainties. This allows realistic interpretation of the solution and the ability to determine the control that individual measurements have over the optimal solution (Norris et al., 2014). This study uses the most recent US EPA version, PMF5, which uses the multilinear engine ME2 to solve the following equation set (Norris et al., 2014):

$$X = G \cdot F + E \quad , \quad x_{ij} = \sum_{p=1}^{q} g_{ip} \cdot f_{pj} + e_{ij} \quad ; \tag{3}$$

$$Q = \sum_{i=1}^{n} \sum_{j=1}^{m} \left(\frac{e_{ij}}{u_{ij}}\right)^2 \quad ,$$

where X is the n by m matrix of measurements with associated uncertainties u, G is the calculated n by q matrix of factor contributions, F is the calculated q by m matrix of factor compositions, E is the n by m error matrix, with lower case variables representing the specific value therein for the i^{th} sample of the j^{th} analyte for the p^{th} factor, and Q is the object function.

So, for any dataset with n measurements of m analytes a solution is found for the matrices G and F for a particular number of factors, p, which produces the minimum value of Q, an optimization parameter calculated as the summed residual error, e, weighted by the measurement uncertainty, u. The Q value can be calculated via two different modes: true (Q_{true}) or robust (Q_{rob}). These modes are identical except that the robust mode of analysis excludes measurements from the calculation of Q if they have a e_{ij}/u_{ij} value greater than 4; thus, the robust mode reduces the impact of outliers. The robust mode was used for this analysis as it is better suited for environmental data which may not be normally distributed (Norris et al., 2014). An additional 10% uncertainty was applied to all measurements in the PMF analysis, beyond that uncertainty captured in Eq. 1, to account for extra modelling uncertainty and further reduce the impact of noise. Any missing measurements were replaced with the median measured value (Norris et al., 2014).

Selection of the number of factors is a critical step of a PMF analysis. Trial runs ranging from 2 to 9 factors were completed using 100 distinct random seeds per run. This study used five considerations during the selection of an optimal number of factors. Firstly, the improvement in Q_{rob} observed with the addition of a factor was calculated. The addition of another factor

Atmos. Chem. Phys. Discuss., https://doi.org/10.5194/acp-2017-718
Manuscript under review for journal Atmos. Chem. Phys.
Discussion started: 14 August 2017

should improve the calculated Q_{rob} value to be considered a viable factor. Secondly, the solution's Q_{rob} was compared to the expected value of Q, calculated as follows (Norris et al., 2014):

$$Q_{exp} = nm - (pn + pm) \quad , \tag{4}$$

where Q_{exp} is the expected value of Q and all other variables are as described in Eq. 3, considering only strong analytes. A ratio of Q_{rob} to Q_{exp} of one was considered ideal. Thirdly, the reproducibility of the solution was examined such that solutions with greater reproducibility among the 100 seeded calculations for each run were given more consideration. Fourthly, the fit of each potential solution was considered. The residuals of each analyte were examined for each potential solution to ensure that they were normally distributed and with a minimal number of normalized residual values greater than 3 across all samples and analytes. Also, the correlation of predicted and measured values was calculated for all analytes. Finally, the interpretability of each solution was considered. Only solutions which produced factor profiles which could be explained in a real-world setting were considered.

The selected optimal solution was repeated with the number of seeds increased to 500 to insure detection of the global minimum and the rotational ambiguity of this solution was then considered. For a given solution, there are several possible G and F matrices defined as rotations of the original solution. The rotation which produced the minimum value of Q was found. Furthermore, G-space plots, which compare the contribution of individual factors to each sample, where examined for the various rotation options. The factors identified by a solution should be independent, i.e., show no relationship on a G-space plot. Also, random error and rotational ambiguity of the PMF solution were quantified using a bootstrap error model with the default parameter settings: block size = 4, number of bootstraps = 50, and minimum correlation R-value = 0.6. Three error models are available with PMF5, but the bootstrap model has been recommended for data where the uncertainties are not well-known (Paatero et al., 2014).

The number of measurements included, n, was limited to dates with sufficient snowfall to complete the majority of analyses. Given the limited number of snow samples measurements available, a subset of the analyzed chemical species was used for PMF analysis. Only analytes with over 60% of measurements above MDL and strong S/N were included in the analysis. Analytes of particular interest to this study with sufficient S/N but only 30-60% of measurements greater than MDL were included in some cases but defined as weak variables (i.e., user-defined uncertainty was tripled for these analytes). Analytes which duplicated others were also excluded from the PMF analysis, such as analytes measured by two methods (e.g., IC and ICP-MS overlapping analytes) and analytes which are expected to share a common source and show extremely strong correlations (e.g., crustal metals with no significant anthropogenic source). Duplicate and closely related analytes do not provide additional information to the apportionment study but artificially inflate the importance of these analytes and increase the ratio of analytes to measurements unnecessarily. The complete list of chemical species included in each analysis is provided with the results.

The relatively small number of samples available for this study was a concern, despite analyte exclusion. Therefore, a simplified supplementary principal component analysis (PCA) was completed to corroborate the PMF results. PCA has been described in detail by others (e.g., Henry et al., 1984). Briefly, PCA describes the measured data as a set of eigenvectors,

termed principal components, which each describe a portion of the observed variance. These eigenvectors and their associated eigenvalues were calculated from the correlation matrix of the measured analytes. There is no non-negativity constraint on the principal components identified by PCA as there is for PMF, nor does PCA provide quantitative factor loadings. Furthermore, PCA does not include measurement weighting by uncertainty and is therefore more sensitive to missing and below MDL values than PMF. Thus, the results of PCA are less conducive to realistic interpretations and were used only as validation of the PMF results. No rotation or error estimates were made for the PCA.

2.4.2 Transport Modelling

The Lagrangian particle dispersion model FLEXPART, described in detail by Stohl et al. (2005), has been shown to be an effective tool for the prediction of transport pathways into and within the Arctic (e.g., Stohl, 2006; Paris et al., 2009). This potential emission sensitivity analysis was completed to identify likely source locations, as a complement to the PMF descriptions of source type. Modelled tracers were initialized over Alert and tracked backwards in time over a ten-day period at a 3-hr time step, driven using operational analysis data from the European Centre for Medium-Range Weather Forecasts with a horizontal resolution of 0.25° in longitude and latitude and 137 vertical hybrid pressure levels. Tracers were initialized at four altitudes over Alert: 100 m, 500m, 1000 m, and 2000 m above sea level. A simulation was completed for every 5 days over the campaign. Simulation results provided the expected residence time of the tracers at the horizontal resolution of the meteorological input data and on 10 levels up to 10 km.

The potential FLEXPART source regions associated with each PMF factor were identified. The peak periods associated with each factor, selected as the top 90th percentile of the factor contribution time series, were used to weight the FLEXPART ten-day residential times over the campaign , as per Eq. 5:

$$t_p^{xy} = \frac{\sum_{i=1}^{n} g'_{ip}\, t_i^{xy}}{\sum_{i=1}^{n} g'_{ip}} \quad (5)$$

$$g'_{ip} = g_{ip} \;\; , if\; g_{ip} \geq g_p^{90} \;\; else, \;\; g'_{ip} = 0$$

where t_p^{xy} is the residence time at location x,y for pth PMF factor, t_i^{xy} is the ith residence time at location x,y, g_{ip}' is the 90th percentile contributions of the pth factor at time i, g_p^{90} is the 90th percentile of g_p, and all other variables are as per Eq. 3.

Only trajectories within 500 m of ground level were considered, given that low-altitude air masses are much more likely to show the influence of ground-level sources; however, selection of this 500 m cut-off height was found to have a negligible impact as the identified potential source regions were similar if it was adjusted in a sensitivity analysis by± 300 m. The weighted sum was then plotted to depict regions which likely influenced each factor.

Atmos. Chem. Phys. Discuss., https://doi.org/10.5194/acp-2017-718
Manuscript under review for journal Atmos. Chem. Phys.
Discussion started: 14 August 2017

3 Results and Discussion

3.1 Selection of Optimal Solution

Positive matrix factorization (PMF) was completed on 49 measurements of 20 analytes in Arctic snow. Three metrics were considered as the basis for this analysis: snow concentration, flux per day, and flux per snowfall (i.e., assuming each sample represented a single snowfall event regardless of the time period over which it occurred, which is known to be true for the majority of samples based on Alert station operator records). Identical PMF analyses were completed for all three metrics, and it was found that the factor profiles identified by all three metrics showed excellent agreement, with Pearson's correlation coefficients above 0.95 for all factors; however, factor contributions varied across the metrics, with correlations as low as 0.35. This is as expected, since the relative variation between analytes does not change with the use of different snow metrics, but the time series should change given that the metrics represent different physical phenomena. The source contributions identified by the flux per snowfall period analysis were the most readily interpreted as physically realistic factors. Moreover, this metric showed the largest correlation between BC snow and atmospheric measurements (Pearson's correlation coefficients of 0.4, 0.3, and 0.5 for BC concentration, flux per day, and flux per snowfall period, respectively), implying that the flux per snowfall may in general be more closely related to the change in analyte sources over time while concentration and flux per day may be more intrinsically dependent on changes in deposition processes. Snow flux per snowfall period results will be presented in the following sections; however, concentration and flux per day results are available in the Table S1 and S2.

Based on the criteria outlined in section 2.4.1, the seven-factor solution was found to be optimal. The seven-factor solution produced one of the largest Q_{rob} improvements with the addition of a factor, an acceptable Q_{rob}/Q_{exp} value, and good reproducibility. In particular, the seven-factor solution showed a marked improvement in fit and interpretability over solutions with fewer factors. The seven-factor solution reproduced measurements with a Pearson's correlation coefficient above 0.8 for all strong analytes. The four, six, and seven-factor solutions all provided readily interpretable source profiles, but the seven-factor solution was considered the most realistic. Furthermore, a repeat run using 500 seeds showed the seven-factor solution to be consistent and stable. The supplemental section S2 provides additional details on solution selection and the evolution of factor profiles over the completed runs. A brief overview of the results of the four and six-factor solutions is provided in the supplemental, as these solutions also showed merit as realistic apportionments of the data.

Rotations were explored for the selected solution with FPeak values of -1.5, -1, -0.5, 0.5, 1, and 1.5, though only the -0.5 and -1 runs were found to converge. However, G-space analysis of the base and rotated solutions showed no improvement with rotation nor did Q_{rob} values or interpretability of the solution improve; therefore, the unrotated base solution was selected. The final solution statistics were: Q_{rob} = 355, Q_{exp} = 329, Q_{rob}/Q_{exp} = 1.08, stability = 94%, and median predicted/measured correlation = 0.94. The input and model diagnostic parameters for each analyte included in this PMF analysis are provided in Table 1. Only the portions considered as insoluble for metals measured by ICP-MS were included in this analysis (Al, V, Cu, As, Se, Sb, and Pb). Residuals of all analytes were found to be normally distributed, based on PMF5's Kolmogorov-Smirnoff test, with the exception of NO_3^- and V, although both appear visually to be close to a normal distribution.

Atmos. Chem. Phys. Discuss., https://doi.org/10.5194/acp-2017-718
Manuscript under review for journal Atmos. Chem. Phys.
Discussion started: 14 August 2017

Table 1: Overview of PMF seven-factor solution input and diagnostic properties.

Analyte	Input Properties			Diagnostic Properties		
	MDL (ppb)	Missing Data	Data Below MDL	Predicted/ Measured Fit	Normalized Residual Mean	Normalized Residual Deviation
Strong Analytes						
BC	0.042	0%	0%	1.00	0.01	0.20
ACE	4.4	0%	4%	0.90	0.08	0.85
FOR	1.2	0%	0%	0.83	0.13	0.77
Cl^-	18	0%	0%	0.96	0.03	0.43
NO_3^-	5.0	0%	4%	0.99	0.01	0.22
SO_4^{2-}	18	0%	0%	0.99	0.01	0.20
Na^+	18	0%	4%	0.99	0.02	0.38
NH_4^+	5.0	0%	2%	0.85	0.07	0.65
K^+	5.0	0%	12%	0.77	0.25	1.11
Mg^{2+}	18	0%	22%	0.95	0.03	0.54
Al	30	8%	27%	0.99	0.00	0.42
V	0.027	8%	10%	0.97	0.09	0.57
As	0.010	8%	0%	0.93	0.09	0.76
Se	0.084	8%	16%	0.99	0.01	0.43
Sb	0.013	8%	0%	0.87	0.17	0.95
Pb	0.16	8%	8%	0.97	0.05	0.67
Weak Analytes						
MSA	1.9	0%	73%	0.70	0.11	0.53
Br^-	5.0	0%	53%	0.46	0.09	0.49
$C_2O_4^{2-}$	18	0%	63%	0.76	0.01	0.18
Cu	0.23	8%	20%	0.49	0.13	0.55

Notes: ACE = acetate; FOR = formate; MSA = methanesulphonate. Predicted/Measured fit presented is Pearson's correlation coefficient. Metals with a charge are those measured by IC, others are insoluble portions measured by ICP-MS.

3.2 Factor Discussion

The profiles and contributions of each identified factor are discussed in the following section. Error estimates provided for the percent apportionment of each analyte are the 25th and 75th bootstrap analysis percentiles. The bootstrap analysis correctly mapped over 96% of sub-sampled data for each factor, with the exception of Factor 7 which was correctly mapped for 76% of the bootstrapped runs. Furthermore, sensitivity runs and PCA analysis all corroborated the presented results. Details on the solution sensitivity and validation analysis are provided in the supplemental. The possible identities of each factor were suggested based on their composition, time series, correlations with non-apportioned analytes (i.e., an analyte which was excluded from the PMF analysis) or with other measured parameters such as meteorology, and source regions.

3.2.1 Factor 1: Marine Sea Salt

The first factor was characterized by high loadings (>75%) of Na^+ and Cl^- and 30-45% loadings of Br^-, K^+, and Mg^{2+} (Figure 1). These compounds are all typical of sea salt, suggesting a marine origin for Factor 1. The composition of Factor 1 was found to be consistent with that of sea salt (Pytkowicz and Kester, 1971). Comparison of modelled and expected loadings of marine

compounds relative to Na^+ found enrichment ratios close to unity: 1.3, 1.7, 1.6, and 1.1 for Cl^-, SO_4^{2-}, Mg^{2+}, and K^+, respectively. The only sea salt compound which was notably different from expected marine levels was Br^- with an enrichment ratio of 3.4, which may indicate aerosol enrichment of Br^- relative to Na^+ or may be a result of this analyte's high uncertainty and poor signal-to-noise. Finally, by taking the ratio of equivalence fluxes calculated for all apportioned ions measured by IC, a neutralization ratio of 0.80 was calculated for this factor (i.e., $[Na^+ + NH_4^+ + K^+ + Mg^{2+}]$ / $[MSA + ACE + FOR + Cl^- + Br^- + NO_3^- + SO_4^{2-} + C_2O_4^{2-}]$, all as equivalence/$m^2$/period), suggesting that the marine aerosol deposited to the surface was neutral.

Factor 1 showed sporadic peaks throughout the campaign, with the largest peak early January (Figure 2). The January peak coincided with a local blizzard, which is consistent with increased sea spray due to windy conditions. Further to this point, the time series of Factor 1 was found to have a slight correlation with local wind speeds, with a Pearson's correlation of 0.3. A dependence on wind speeds might also indicate a potential frost flower source to this factor, given the strong correlation between winds and salt emissions from fresh sea ice frost flowers which has been observed by others (e.g., Xu et al., 2013). No non-apportioned analyte showed significant correlation with Factor 1. Weighting the FLEXPART predicted source areas by the Factor 1 peak dates (Figure 3) showed the Eurasian coast of the Arctic Ocean, which remains ice-free for a long portion of the winter, to be a likely source of sea salt to Alert. The Norwegian Sea and northern Atlantic Ocean were also highlighted as potential sources of sea salt to Alert.

The marine factor was found to be highly robust over this apportionment analysis. All runs with more than two factors exhibited a resolved Na/Cl-dominated factor, and the composition of this marine factor was found to be maintained across each addition of a new factor with Pearson's correlation coefficients above 0.98. Bootstrapping analysis found little error associated with this factor. Furthermore, similar marine factors have been observed in previous apportionment studies of Arctic snow (Hegg et al., 2009; Hegg et al., 2010) and Arctic aerosol (Sirois and Barrie, 1999; Nguyen et al., 2013). Therefore, Factor 1 was identified as primarily marine in origin based on its agreement with typical sea salt composition. This factor was found to be weakly related to wind speeds, possibly indicating increased salt emissions of frost flowers and sea spray, and largely originating in the ice-free areas of the Arctic Ocean and northern Atlantic.

Atmos. Chem. Phys. Discuss., https://doi.org/10.5194/acp-2017-718
Manuscript under review for journal Atmos. Chem. Phys.
Discussion started: 14 August 2017

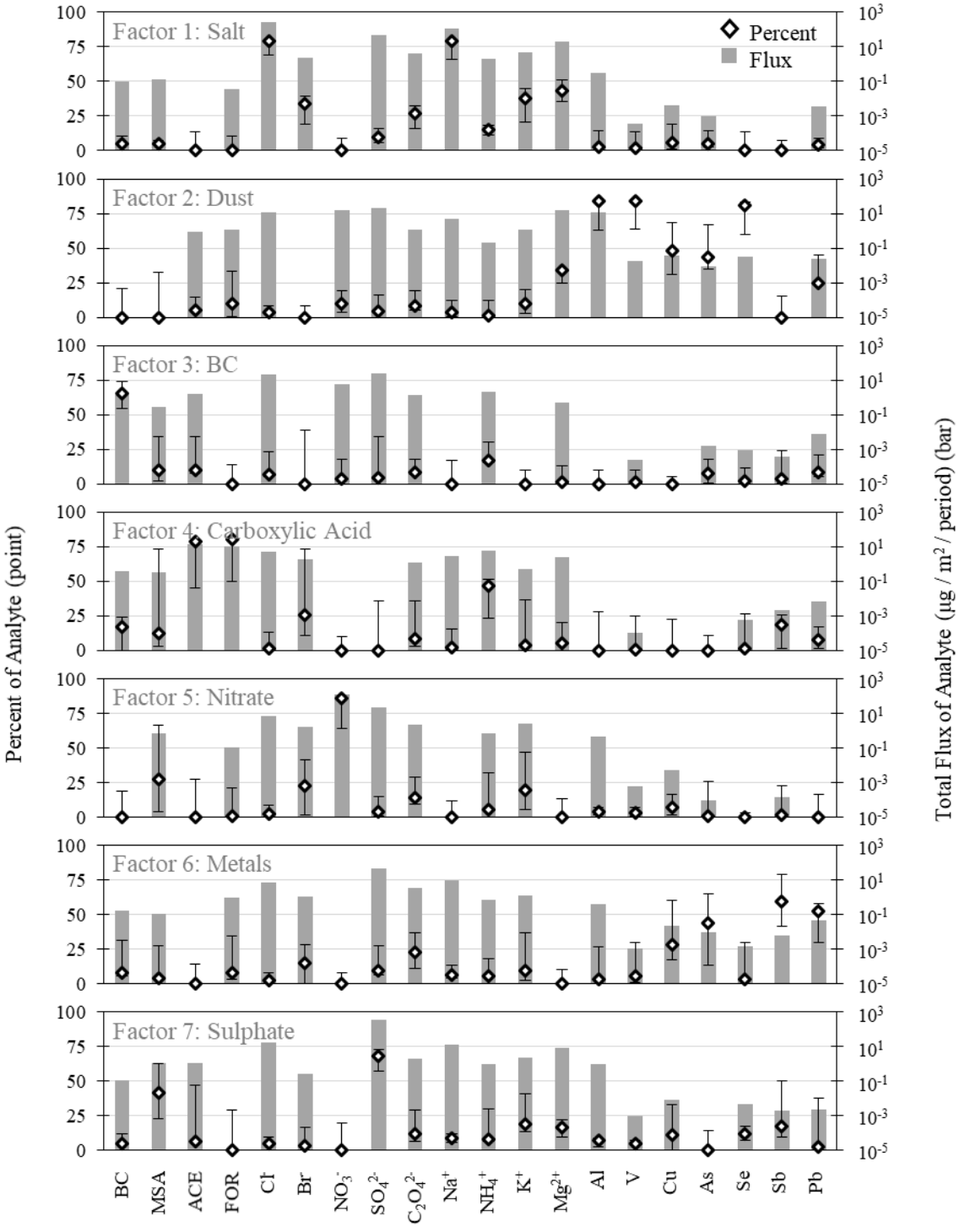

Figure 1: Factor profiles. Error bars show the 25th and 75th percentiles of the bootstrapping analysis. Flux contributions below 0.00001 µg/m²/period are not shown.

Atmos. Chem. Phys. Discuss., https://doi.org/10.5194/acp-2017-718
Manuscript under review for journal Atmos. Chem. Phys.
Discussion started: 14 August 2017

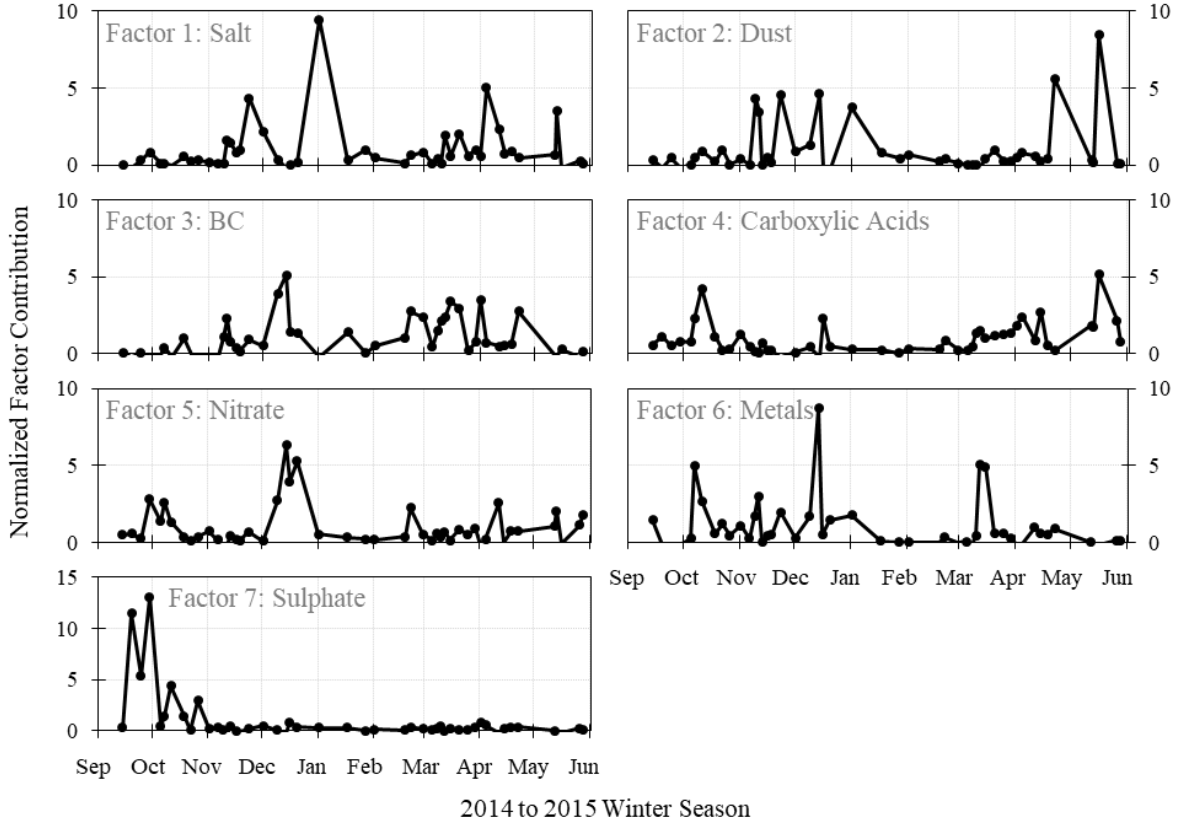

Figure 2: Normalized factor contributions.

3.2.2 Factor 2: Crustal Metals

Factor 2 was characterized by elevated levels of Al, V, and Se, all over 80% loading, and 25-50% loading of Cu, As, Mg^{2+}, and Pb (Figure 1). All of these metals suggest a crustal origin for this factor. The composition of dust is far more variable than that of sea salt. Thus, no single enrichment ratio can be determined for each analyte loaded on to Factor 2; however, the modelled ratios of Al to Mg^{2+}, K^{+}, V, Cu, As, Se, Sb, and Pb all appear realistic when they are compared with a variety of crustal sources, with calculated enrichment ratios in the range of 1 to 15 (Taylor, 1964; Barrie, den Hartog, and Bottenheim, 1989; Masson-Delmotte et al., 2013). Specifically, the modelled ratio of As/Al was seen to be closer to that of local soils (Barrie, den Hartog, and Bottenheim, 1989) than the global typical composition (Taylor, 1964; Masson-Delmotte et al., 2013) with enrichment ratios of 6 and 37, respectively. The composition of the Crustal Metals Factor suggested an alkaline aerosol with a neutralization ratio of 1.5, calculated as described in section 3.2.1.

Atmos. Chem. Phys. Discuss., https://doi.org/10.5194/acp-2017-718
Manuscript under review for journal Atmos. Chem. Phys.
Discussion started: 14 August 2017

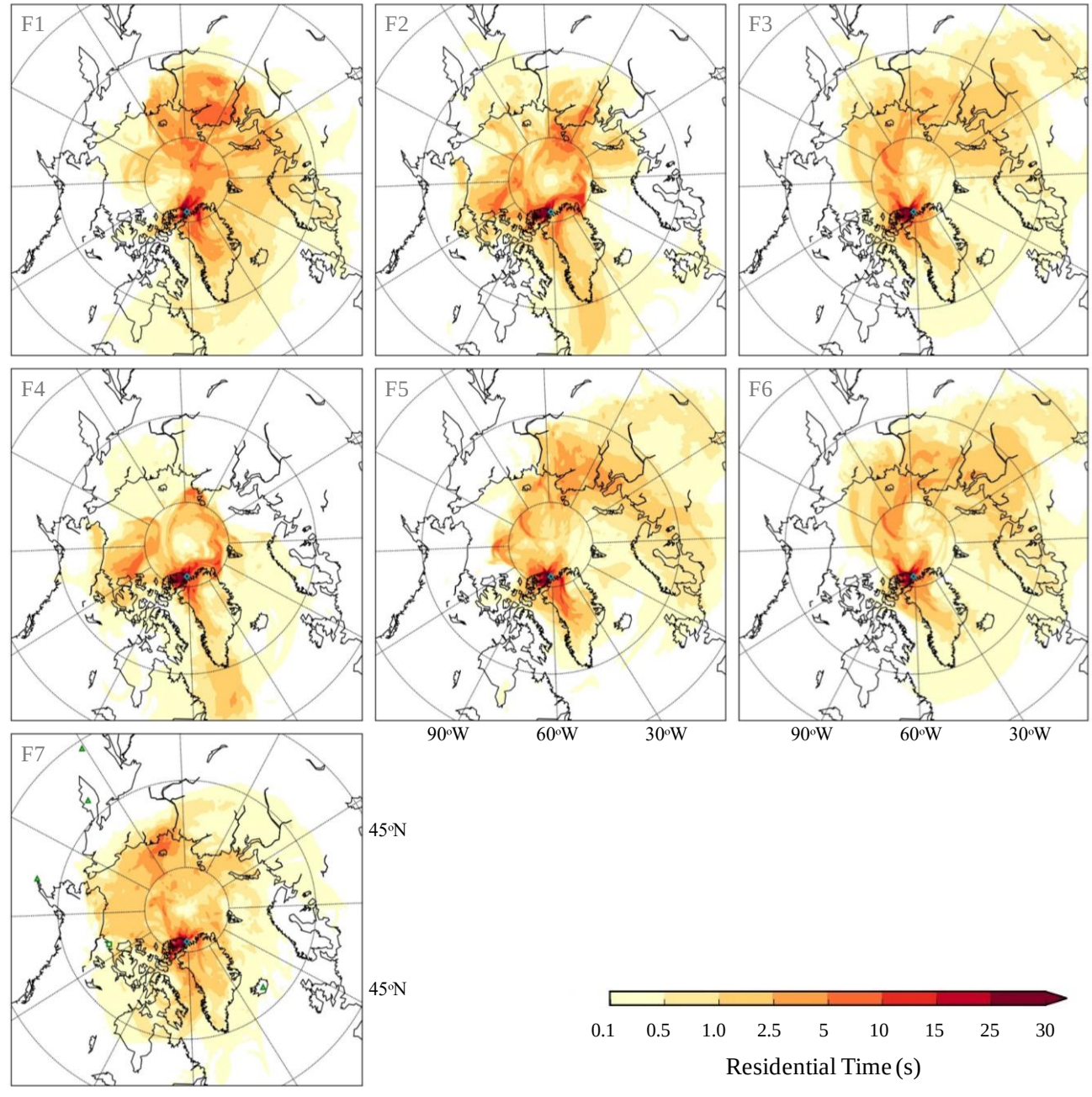

Figure 3: Potential source regions of apportionment factors (F1 to F7). Cyan diamonds on plot shows the location of Alert, Nunavut. Factor 7 plot depicts active volcanoes as green triangles, and the Smoking Hills as a green square (Hunter, 2007).

The Crustal Metals Factor showed sporadic peaks over the campaign but primarily from November to February and after April. This time series showed good agreement with non-apportioned metals typically considered to be dominated by crustal origins: insoluble Fe, Mn, Co, Tl, and Ca. The time series of this factor also showed slight correlations with winds from the direction

of the base camp and winds speeds, with Pearson's correlations of 0.39 and 0.26, respectively. This, along with the calculated As/Al ratio, suggest that this crustal factor may be dominated by local soil and dust, likely from cleared or paved areas at the Alert base camp. The potential source regions calculated from FLEXPART results for this factor are shown in Figure 3. Arctic areas dominate the identified potential source region, again suggesting local soils were a major contributor to this factor; however, potential long-range sources of northern Asia, North America and Atlantic Ocean were also identified. A primarily local dust source is supported by the findings of Zwaaftink et al. (2016), which showed that surface dust loads within the high Arctic are typically dominated by Arctic sources with an annual average contribution of 78% by concentration or 70% by deposition from sources above 60 °N.

A factor dominated by crustal metals was consistently resolved among the completed apportionment runs. This factor maintained a fairly similar composition across all numbers of factors, with Pearson's correlation coefficients above 0.97. However, metals traditionally considered to be associated with industrial activities, such as Pb, Cu, As, and Sb, were observed to gradually split from this factor with the addition of new factors. The seven-factor solution for this factor showed low levels of error according to the bootstrapping analysis. Similar factors have been observed in previous atmospheric apportionment studies (e.g., Sirois and Barrie, 1999; Nguyen et al., 2013) but typically were not seen to account for such a large percentage of these metals, i.e., with loadings of 25-60% for major crustal analytes. This might suggest that a separate source was missed by this study, though this seems unlikely given the consistency of the observed factor. Sirois and Barrie (1999) found the crustal signature at Alert to be dominated by local sources during the fall and long-range transport in the late spring to summer. This supports a single local source for this study of the winter season, while studies of the full year may have split crustal analytes among various long-range transport sources. However, the April-May peak in the crustal factor observed in this study coincides with Sirois and Barrie's (1999) peak considered to be dominated by long-range dust transport.

Based on the loading of crustal metals, Factor 2 was identified as a crustal source. The composition of this factor resembled that of local Alert soil and the correlation with base camp winds and FLEXPART results support a local origin to this factor. However, previous studies have shown mixed agreement on the dominance of local crustal sources within the Arctic over dust transported from lower-latitudes.

3.2.3 Factor 3: Black Carbon

The third factor was characterized by a high loading of BC, 66% of the total BC, with all other analyte loads below 20% (Figure 1). Most conspicuous was the absence of K^+, considered to be a tracer of biomass burning which can be a significant source of BC. Furthermore, the ratios of SO_4^{2-} and NO_3^- to BC were much higher than would be expected for biomass burning with enrichment ratios above ten (Turn et al., 1997; Hays et al., 2005; Saarikoski et al., 2007; McMeeking et al., 2009). Factor 3 also exhibited a moderate NH_4^+ loading of 17%. While NH_4^+ is more commonly associated with agricultural emissions, it can also be produced by biomass burning, vehicle emissions, and some industrial activities (Behera et al., 2013). This factor also showed an acidic signature with a neutralization ratio of 0.12, which suggest an industrial rather than biomass burning source.

The Black Carbon Factor showed an enhanced contribution over the Arctic Haze season, November through April (Figure 2). The time series of this factor did not show a significant correlation with any non-apportioned analyte; however, it did show weak correlations with insoluble Ti and Tl and inverse correlations with temperature and humidity. Also, the peaks in this factor did not coincide with dates of known northern hemisphere forest fire activity (as per fire records of NASA Global Fire Maps, retrieved May 2016 from https://lance.modaps.eosdis.nasa.gov). Further to this point, the observed winter peak of this factor did not suggest any significant contribution from forest fires which are more prevalent in warmer months. Weighting of FLEXPART results by peak periods for Factor 3 indicated that Eurasia was a probable source of this factor (Figure 2), especially northern Russia and some portions of central southern Russia. These source regions correspond with known flaring and industrial BC sources (in the vicinity of the Ob and Pechora rivers and the Taymyrsky Dolgano-Nenetsky District, respectively) (Huang et al., 2015). A BC-dominated factor was resolved for all runs with four or more factors, and its composition remained consistent with Pearson's correlation coefficients of 0.95 or greater. Thus, the practically unique origin of BC was fairly robust through this analysis. Furthermore, the loading of non-sea salt (NSS) K^+ onto all resolved BC-dominated factors was below 12%, suggesting that a primarily biomass burning origin to BC was unlikely. Based on the elevated SO_4^{2-} levels, the mid-winter peaks, and the Eurasian source region, Factor 3 appears to be predominantly the product of anthropogenic fossil fuel burning, though likely contains a mixture of Eurasian sources: industrial, urban, residential burning, and other minor contributors.

There has been considerable disagreement among previous studies on the dominant source of BC to the Arctic. Several modelling studies have suggested that combined anthropogenic sources (fossil fuel and biofuel burning) account for 75-96% of BC in Arctic snow, especially elevated over the winter months with spring and summer proportions dependent on the frequency of forest fires of that year (Flanner et al., 2007; Skeie et al., 2011; Wang et al., 2011; Xu et al., 2017). A recent study by Xu et al. (2017) analysing airborne measurement from a similar time period as this study found about 90% of BC to likely be anthropogenic in source, primarily from Eurasia. In particular, modelling studies have shown winter Arctic BC to be dominated by flaring and other mixed industry emissions, with less impact from anthropogenic biomass (often termed biofuel) burning (Flanner et al., 2007; Stohl et al., 2013). Similarly, studies of Arctic snow composition have suggested that over 85% of BC is from the combustion of fossil fuels, based on radiocarbon analysis and measured ratios with biomass burning tracers (Slater et al., 2002; Yttri et al., 2011; Yttri et al., 2014). In contrast, previous apportionment studies of Arctic spring snowpack have attributed over 90% of BC to biomass burning origins (Hegg et al., 2009; Hegg et al., 2010). These contradicting snow BC apportionment findings may be the result of spatial and temporal differences between this and previous studies, specifically the stronger focus on low Arctic locations and spring sampling within these previous studies. Although high Arctic winter snow samples were sparse in previous apportionment studies, the few available showed an enhanced fossil fuel signature, though over 30% of BC at these sites was still attributed to biomass burning (Hegg et al., 2010). This smaller discrepancy cannot be satisfactorily explained by the annual variability in biomass burning intensity, as both study periods were found to represent fairly typical years in Northern hemisphere biomass burning emissions (Global Fire Emissions Database, version 4.1, retrieved July 2016 from http://www.globalfiredata.org). Table 2 summarizes the apportionment of BC by the studies

discussed above. Overall, the loading of winter BC onto one major source with a largely fossil fuel combustion origin is generally in agreement with previous modelling and snow composition studies, though unexpectedly different from some previous snow apportionment studies.

Table 2: Overview of BC apportionment studies.

Analysis	Study	Description	BC Apportionment (%)		
			FF	BF	BB
Co-Variance	This Work	Temporally-refined snow PMF	73%	↔	17%
	Hegg et al. 2009	Spatially-refined snow PMF	7%	→	93%
	Hegg et al. 2010	Spatially-refined snow PMF	6%	→	90%
Model	Flanner et al. 2007	SNICAR + general circulation model	60-70%	20%	10-20%
	Skeie et al. 2011	Oslo CTM2 model	85-95%	←	5-15%
	Wang et al. 2011	GEOS-Chem CTM	45-60%	15-35%	10-40%
	Xu et al. 2017	GEOS-Chem (global, spring)	90%	↔	10%
Composition	Slater et al. 2002	Radiocarbon	60-100%	→	0-40%
	Yttri et al. 2011	Radiocarbon	>95%	→	<5%
	Yttri et al. 2014	Levoglucosan ratio	85-95%	→	5-15%

Notes: FF = Fossil fuel, BF = Biofuel, BB = Biomass burning. Arrows indicate when BF has been grouped in with FF and/or BB.

3.2.4 Factor 4: Carboxylic Acids

Factor 4 was characterized by high loadings, 79-80%, of acetate (ACE) and formate (FOR); moderate loadings, 25-50%, of NH_4^+ and Br^-; and lower loadings, 10-20%, of Sb, BC, and MSA (Figure 1). The loadings of Br^- and MSA on this factor were highly variable, as shown by the bootstrap results in Figure 1; however, both of these analytes had high associated uncertainty. The composition of this factor suggested a neutral aerosol with a neutralization ratio of 1.02. Factor 4 exhibited peaks in October and May (Figure 2) and was seen to moderately correlate with propionate, hours of sunlight, and base camp winds, with Pearson's correlation coefficients of 0.4-0.5. Weighted FLEXPART results indicated a local, North American, and/or Atlantic Ocean source for this factor. A variety of potential source may have contributed to this factor but the available evidence does not allow a robust identification. Possible contributors hypothesized in other studies of arctic carboxylic acids are discussed below including biomass burning, atmospheric or snow photochemical processing, and ocean microlayer emissions. However, some studies have postulated the existence of a yet unidentified source of high-latitude carboxylic acids (e.g., Paulot et al., 2011) which may be reflected in Factor 4. A similar high carboxylic acid factor was resolved for runs with six or greater factors and maintained its composition with Pearson's correlation coefficients of over 0.96; however, the loading of BC and K^+ onto this carboxylic acid factor was much more variable over the additional runs.

Carboxylic acids within the Arctic have previously been linked with both biomass burning plumes (e.g., Jaffrezo et al., 1998; Legrand and de Angelis, 1996). The ratio of BC and K^+ apportioned to this factor was similar to that of a biomass burning plume, particularly to the high K^+ proportion typical of herbaceous burning (Turn et al., 1997; Saarikoski et al., 2007; McMeeking et al., 2009); however, both BC and K^+ loading showed significant uncertainty. The loadings of formate, acetate, Cl^-, Br^-, $C_2O_4^{2-}$, and NH_4^+ appeared to be higher than expected for biomass burning emissions: the ratio of these analytes to BC were enriched by a factor of 3 to 40 relative to typical ratios of biomass burning emissions, based on a review of measured herbaceous and woody emissions (Turn et al., 1997; Andreae and Merlet, 2001; Hays et al., 2005; Saarikoski et al., 2007; McMeeking et al., 2009). The observed enrichment ratios of this factor above typical biomass burning plumes could be explained by atmospheric processing, for example, the cloud processing suggested by Legrand and de Angelis (1995). Alternatively, gas-phase partitioning and the subsequently enhanced scavenging observed in a previous study of this data (Macdonald et al., 2017) may have led to increased levels of some co-emitted chemical species relative to BC. The fall and spring peak of Factor 4 may support a biomass burning identification, as burning events are more typical in warmer seasons, specifically a North American source as suggested by the FLEXPART analysis.

Previous studies have also suggested a photochemical processing source of these carboxylic acids in the Arctic. Dibb and Arsenault (2002) found elevated levels of formic and acetic acid in the pore space of deposited Arctic snow and hypothesized oxidation of carbonyls and alkenes within the snowpack as a likely source. The prevalence of the factor in the fall and spring, before polar sunset and after polar sunrise, would support a photochemical source. Furthermore, summertime measurements of Arctic atmospheric samples by Mungall et al. (2017) also showed high levels of formic and acetic acid. This study hypothesized an oceanic microlayer photochemical source. Again, the temporal trend of Factor 4 as well as the Atlantic Ocean source location would support this possibility. An atmospheric budget analysis by Paulot et al. (2011) identified a significant missing source of high-latitude formic and acetic acid. Factor 4 of this study could represent a combination of the suggested sources above, or a missing source which is as yet unidentified.

3.2.5 Factor 5: Nitrate

The fifth factor was characterized by high NO_3^-, 86% loading (Figure 1). This factor was also seen to have moderate loadings of MSA and Br^-, 20-30%, but with a larger degree of uncertainty. The atmospheric chemistry of NO_3^- is complex, involving a variety of sources, formation mechanisms, and destruction mechanisms; in particular, snow can act as both a sink and a source of atmospheric nitrogen oxides, further complicating the local NO_3^- cycle (Morin et al., 2008; Fibiger et al., 2016). Furthermore, the complex processing of NO_3^- was demonstrated in the earlier deposition analysis of this data which suggested that gas-phase deposition was a dominant mechanism of NO_3^- transport into snow (Macdonald et al., 2017). Thus, the loading of NO_3^- onto a separate factor may be a reflection of its unique atmospheric processing. This NO_3^--loaded factor was resolved for simulations with six or greater factors, prior to which this factor appears to be combined with the carboxylic acid factor. In addition, a similar unique NO_3^- factor was also observed in previous snow and atmospheric apportionment studies (Sirois and Barrie, 1999; Hegg et al., 2009; Hegg et al., 2010).

Factor 5 showed a variable contribution throughout the campaign but especially elevated in December. This factor was not found to correlate significantly with any non-apportioned analyte or meteorological parameter; however, Factor 5 did weakly correlate with nitrite (NO_2^-) and H^+ with Pearson's correlation coefficients of 0.35 and 0.46, respectively. This correlation with H^+ is in agreement with this factor's low neutralization ratio of 0.04. The low fall/spring levels of this factor may reflect the loss of NO_3^- from snow through photolysis driven by the sunlight availability after polar sunrise (Morin et al., 2008; Fibiger et al., 2016). The highest NO_3^- levels were observed when photolysis is inhibited during the polar sunset from mid-October to late-February. The movement of NO_3^- accumulated in the snow to atmosphere during the spring is supported by the broad peak in atmospheric NO_3^- observed via Hi-Vol filters from February to the end of the atmospheric sampling in mid-May. February to June, 2015, was also characterized by a "bromide explosion", observed as a broad peak in snow and atmospheric Br^-. It is possible that this offered a different formation pathway for NO_3^- over this period via the reaction of NO_2 and BrO (Morin et al., 2008). The mid-winter peak in this factor may be linked to NO_3^- formation via NO_3-radical chemistry, which is considered to dominate Arctic NO_3^- chemistry during the night (Morin et al., 2008).

Potential source areas of this factor, largely driven by the December peak, are shown in Figure 2. This plot was found to be similar to that of Factor 3, primarily northern Eurasia, though with a possible stronger dependence on northern Europe. Thus, the NO_3^- precursors to this factor may be largely anthropogenic in origin. Additionally, this factor appears to coincide with increased transport over the ice-free Norwegian Sea and northern Atlantic. This transport pathway might explain the presence of MSA, typically considered an indicator of marine biogenic activity within warmer ice-free water bodies (Li et al., 1993; Ye et al., 2015).

3.2.6 Factor 6: Non-Crustal Metals

Factor 6 showed a high loading of Sb, Pb, and As, 40-60%, and moderate Cu loading, 28%, as shown in Figure 1. These metals are frequently associated with industrial emissions, particularly high-temperature activities such as fossil fuel combustion and smelting (Berg, Røyset, and Steinnes, 1994; Laing et al., 2014). Although total Se and V loadings to this factor are low, the non-crustal loading of these metals (i.e., percentage of total excluding that which is loaded on Factor 2) are 20-30%. This factor also contains 10% of non-sea salt SO_4^{2-}. These constituents also point towards an industrial source (Berg, Røyset, and Steinnes, 1994; Laing et al., 2014). A neutralization ratio of 0.37 for this factor suggested an acidic aerosol. Factor 6 exhibited major peaks in October, December, and March and was found to be associated with a Eurasian source (Figure 2). Although several of the non-apportioned metals had limited measurements above MDL, a possible correlation was observed between Factor 6 and insoluble Ti, Cr, and Tl, and soluble As, Pb, Cr, and Cd. These metals are often considered to be primarily industrial in origin (Berg, Røyset, and Steinnes, 1994; Laing et al., 2014). The similarity in the FLEXPART potential source maps between Factor 3 (BC) and Factor 6 may support their mutual designation as anthropogenic-related.

Factors 6 and 7 were resolved separately only for solutions with seven or more factors. With the addition of a ninth factor, the non-crustal metals factor was further split into a factor dominated by As and Pb and a second factor dominated by Sb. This may represent the resolution of different industrial sources; however, the addition of these factors was not found to greatly

improve the overall solution fit. Factors dominated by non-crustal metals, specifically Pb and As, have been observed in previous atmospheric apportionment studies (Sirois and Barrie, 1999; Nguyen et al., 2013) but not as clearly in existing snow apportionment studies (Hegg et al., 2009; Hegg et al., 2010).

3.2.7 Factor 7: Sulphate

Factor 7 was characterized by SO_4^{2-} and MSA, with loadings of 68% and 42%, respectively (Figure 1). MSA is considered to be a tracer for biogenic marine activity; however, the ratio of MSA/SO_4^{2-} observed in Factor 7, 0.003, is far below that typically seen for marine biogenic emissions, 0.05-0.20 (Li et al., 1993). Thus, an additional source of SO_4^{2-} to this factor was suggested. Several volcanoes within the near Arctic were known to be active over the 2014-15 season: Bárðarbunga, Iceland; Shishaldin, Aleutian Islands; Sheveluch, Bezymianny, and Zhupanovsky, Kamchatka Peninsula; and Chirpoi, Kuril Islands (Global Volcanism Program, retrieved March 2016 from http://volcano.si.edu/). Volcanic emissions are characterized by high levels of sulphur dioxide (SO_2, an oxidation precursor of SO_4^{2-}), acidic compounds, and a variety of metals (AMAP, 2006). A volcanic source would be consistent with the observed low levels of BC and NO_3^- associated with Factor 7, which do not suggest an industrial source. In addition, Factor 7 contained 62% of the non-crustal Se signature and 28% of non-crustal V. Non-crustal Se is typically considered to be a tracer of coal combustion and V a tracer of oil combustion (Laing et al., 2014). The Smoking Hills are located on the northern coast of the Northwest Territories, Canada, at Cape Bathurst, 69.5 °N, 126.2 °W. These hills are a natural phenomenon whereby coal and oil shale deposits within the hills have been combusting for centuries, continuously emitting sulphur and metal aerosols (Freedman et al., 1990; AMAP, 2006). Thus, Factor 7 appeared to be related to natural regional SO_4^{2-} sources: marine biogenic activity and volcanic and/or Smoking Hills activity. The portion of SO_4^{2-} in this factor related to marine biogenic emissions was estimated at about 2-7%, assuming a typical MSA/marine-SO_4^{2-} ratio and similar scavenging of MSA and marine SO_4^{2-}. Also, given the relatively low emissions of the Smoking Hills, a volcanic source is suggested as the dominant origin to this factor.

Factor 7 showed a distinct maximum in September/October and a low contribution throughout the remainder of the campaign. The contribution calculated for this factor correlated well with measurements of the non-apportioned analytes NO_2^-, H^+, and Ba. Acids are a large component of volcanic and Smoking Hill emissions and Ba has been associated with coal burning (Berg, Røyset, and Steinnes, 1994; AMAP, 2006). Furthermore, a neutralization ratio of 0.17 was calculated for this factor suggesting an acidic aerosol. The seventh factor also showed a correlation with temperature and hours of sunlight. This supported both a biogenic/photochemical source, which would be more active in the warmer months, and a volcanic/Smoking Hills source, which would emit SO_2 and require an oxidizing atmosphere for conversion to SO_4^{2-}.

The potential source regions of Factor 7 were dominated by local Arctic areas (Figure 2). In particular, ice-free areas of the Arctic Ocean were found to have a significant impact, supporting a marine biogenic contribution. The Bárðarbunga volcano in Iceland and the Smoking Hills in Canada appeared to be the most probable non-marine sources to this factor. Moreover, Bárðarbunga activity was observed by others to diminish in February 2015 (Icelandic Met Office via Global Volcanism

Program, retrieved March 2016 from http://volcano.si.edu/). This decline in volcanic activity may explain the negligible contribution of Factor 7 observed in the spring, despite the similar transport and meteorological conditions as the fall.

Factor 7 appeared to be predominantly a volcanic source, based on SO_4^{2-} loading, potential source regions, and records of simultaneous volcanic activity. Within a six-factor solution, Factors 6 and 7 are essentially combined into a single factor. This combined factor did not exhibit a clear distinct source region, nor was it easily interpretable. Thus, the use of a seven-factor solution vastly improved SO_4^{2-} apportionment for this campaign. Photochemical SO_4^{2-} apportionment sources have been observed in some previous apportionment studies, though not as commonly as other factors (Sirois and Barrie, 1999).

3.3 Overall Apportionment

An overview of each factor and its proposed identity is provided in Table 3. The total residence time by major region is also presented for each factor. All factors were observed to reside primarily in Arctic source areas, due to the predominant transport of air masses over the Arctic Ocean. The sources associated with BC were of particular interest to this study, due to its importance in the Arctic climate. Although each factor is potentially an amalgamation of several co-emitted or co-aligned sources, evidence has been presented that the dominant source of BC, Factor 3, is primarily the product of fossil fuel combustion. When combined with the BC attributed to the industrial source Factor 6, 73% of BC at this site is found to be predominantly the product of fossil fuel combustion (bootstrapping provides a range of 59%-100%). Although biomass burning has previously been argued as the dominant source of BC to more southern Arctic snow (Hegg et al., 2009; Hegg et al., 2010), only 17% of BC was loaded onto the factor most resembling biomass burning, Factor 4, similar to the findings of previous modelling and composition-based apportionment estimates for particulate matter (Slater et al., 2002; Flanner et al., 2007; Skeie et al., 2011; Wang et al., 2011; Yttri et al., 2011; Yttri et al., 2014). The portions of BC assigned to Factors 1 (Marine Elements), 2 (Crustal Metals), and 7 (Sulphate) likely represent a regional background level of BC and therefore are likely the combined product of both anthropogenic and natural emissions. In general, the apportioned analytes differed in how exclusively they were attributed. Some analytes were found to be predominantly loaded onto a single factor: BC, sea salt, and crustal particles. This may indicate that much of the mass of these analytes exist in externally mixed particles, or internally mixed with a relatively small coating mass. In contrast, other analytes were found to be loaded more evenly onto several factors: MSA, Br^-, K^+, and $C_2O_4^{2-}$. Thus, these analytes may exist primarily as internally mixed particles or gas-phase compounds. This assessment is in agreement with previous explorations in the deposition characteristics of this data (Macdonald et al., 2017).

Although BC was apportioned primarily to Factor 3 overall, its main source changed over the collection campaign. Figure 4 shows the apportionment of BC across the 2014-15 season (Factors 2 and 5 are omitted as they were predicted to have zero contribution to BC). Factor 3 (BC) was dominant from November through April, but Factors 4 (Carboxylic Acids) and 7 (Sulphate) showed larger contributions in the fall and spring. However, given the low levels of BC observed over fall and spring, the absolute contributions of Factor 4 and 7 were small and susceptible to significant uncertainty, as shown in Table 3. In general, most analytes were found to exhibit similar source profiles over the campaign. The most notable variability in

Atmos. Chem. Phys. Discuss., https://doi.org/10.5194/acp-2017-718
Manuscript under review for journal Atmos. Chem. Phys.
Discussion started: 14 August 2017

Table 3: Overview of factor source regions and BC apportionment.

Factor	Dominant Composition	Source Region % Residence Time				BC Loading	Proposed Dominant Identity
		Arctic	North America	Eurasia	Southern Oceans		
1	Na^+, Cl^-	84%	1%	14%	2%	5% [0-10%]	Sea salt
2	Al, V, Se	92%	1%	5%	2%	0% [0-21%]	Regional dust
3	BC	85%	0%	14%	1%	66% [54-74%]	Mixed Eurasian fossil fuel combustion
4	FOR, ACE	94%	2%	1%	3%	17% [0-24%]	Mixed carboxylic acid sources
5	NO_3^-	83%	0%	16%	1%	0% [0-19%]	Eurasian anthropogenic emissions and regional complex processing
6	Sb, Pb, As	82%	0%	17%	1%	8% [5-31%]	Eurasian industrial activities
7	SO_4^{2-}, MSA	91%	3%	6%	1%	5% [0-12%]	Regional volcanic and marine biogenic activity

Notes: "Southern Oceans" are defined as areas of the Atlantic and Pacific below 65 °N. "Arctic" source area includes the northern Pacific/Atlantic Oceans, Arctic Ocean, Canadian high Arctic, and Greenland. BC loading described as: optimal solution [25th - 75th bootstrapping].

source profile were observed for BC, as shown above, and K^+, which was dominated by Factor 7 (Sulphate) during the spring/fall and Factor 1 (Marine Elements) during the winter.

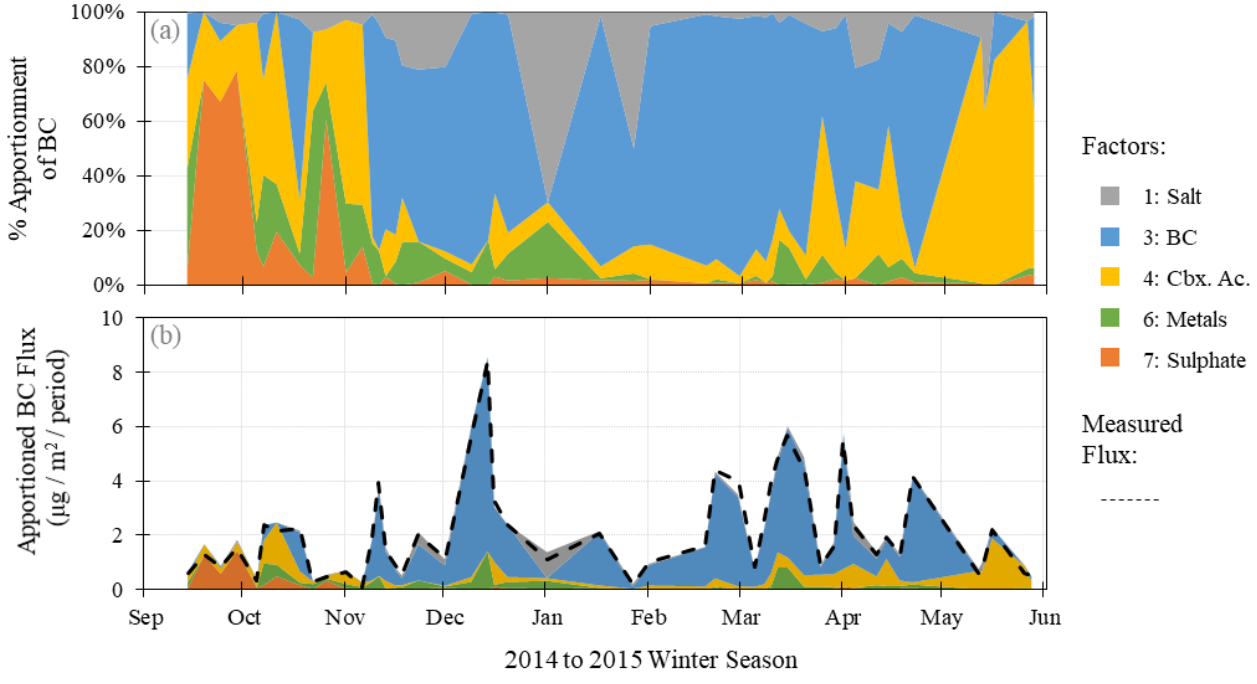

Figure 4: Percent (a) and total (b) apportionment of BC in snow over the 2014/15 campaign.

4 Conclusions

The Arctic climate has undergone significant climate change over recent decades and any effort to control and mitigate these changes requires improved understanding of the source contributing to the Arctic snow burden. The data presented here represents an unprecedented campaign of temporally-refined and broadly speciated snow samples which is the first of its kind to be applied to a detail source apportionment analysis. Positive matrix factorization of the snow measurements was found to resolve seven factors with good solution diagnostics, interpretability, and agreement with measured values. These factors were identified based on composition, seasonally contribution, and FLEXPART-predicted major source regions: sea salt, regional dust, mixed Eurasian fossil fuel combustion, mixed carboxylic acid sources, complex NO_3^- processing, Eurasian industrial activities, and regional volcanic and marine biogenic activity. BC apportionment loaded 73% onto factors considered to be primarily fossil fuel combustion and Eurasian in origin; however, the lower levels of BC in the fall and spring were largely associated with North American biomass burning. These findings are in agreement with previous modelled and compositionally estimated apportionments of BC in the Arctic atmosphere, but disagree with high biomass burning loadings of BC observed in previous snow apportionment studies. A predominance of fossil fuel produced BC in the Arctic, especially within the snow reservoir, could be a critical driver in action plans for mitigating regional climate effects.

Author Contribution

Organization of the snow collection campaign was lead by S. Sharma with the assistance of A. Platt and collection by M. Elsasser. Snow analyses were completed by J. McConnell, N. Chellman, D. Toom, L. Huang, and K. Macdonald with the assistance of A. Chivulescu, Y. Lei, and C.-H. Jeong. Ambient atmospheric monitoring was completed by D. Toom and R. Leaitch. FLEXPART simulations were completed by H. Bozem and D. Kunkel with data analysis assisted by K. Macdonald. PMF analysis was completed by K. Macdonald with input on interpretation from all authors. Dr. G. Evans and J. Abbatt provided oversight for the project, including input on the manuscript.

Competing interests

The authors declare that they have no conflict of interest.

Acknowledgements

Funding of this study was provided as part of the Network on Climate and Aerosols Research (NETCARE), Natural Science and Engineering Research Council of Canada (NSERC), the government of Ontario through the Ontario Graduate Scholarship (OGS), and Environment and Climate Change Canada. This project would not have been possible without the collaboration of

Atmospheric Chemistry and Physics Discussions

many skilled individuals, including Allan K. Bertram and Sarah Hanna at the University of British Columbia and Catherine Philips-Smith at the University of Toronto.

References

AMAP: Acidifying pollutants, Arctic haze, and acidification in the Arctic, Arctic Monitoring and Assessment Programme, Oslo, Norway, 2006.

AMAP: Snow, water, ice and permafrost in the Arctic: Climate change and the cryosphere, Arctic Monitoring and Assessment Programme, Oslo, Norway, 2011.

AMAP: Black carbon and ozone as Arctic climate forcers, Arctic Monitoring and Assessment Programme, Oslo, Norway, 2015.

Andreae, M. O., and Merlet. P.: Emission of trace gases and aerosols from biomass burning, Global Biogeochem. Cy., 15 (4), 955–966, doi:10.1029/2000GB001382, 2001.

Behera, S. N., Sharma, M., Aneja, V. P., and Balasubramanian, R.: Ammonia in the atmosphere: A Review on emission sources, atmospheric chemistry and deposition on terrestrial bodies, Environ. Sci. Pollut. R., 20 (11), 8092–8131, doi:10.1007/s11356-013-2051-9, 2013.

Barrie, L. A., Hoff, R. M., and Daggupaty, S. M.: The Influence of mid-latitudinal pollution sources on haze in the Canadian Arctic, Atmos. Environ. (1967), 15 (8), 1407–1419, doi:10.1016/0004-6981(81)90347-4, 1981.

Barrie, L. A., den Hartog, G., and Bottenheim, J. W.: Anthropogenic aerosols and gases in the lower troposphere at Alert, J. Atmos. Chem., 9, 101–127, doi:10.1007/BF00052827, 1989.

Berg, T., Røyset, O., and Steinnes, E.: Trace elements in atmospheric precipitation at Norweigan background stations (1989–1990) measured by ICP-MS, Atmos. Environ., 28 (21), 3519–3536, doi:10.1016/1352-2310(94)90009-4, 1994.

Bond, T. C., Doherty, S. J., Fahey, D. W., Forster, P. M., Berntsen, T., Deangelo, B. J., Flanner, M. G., et al.: Bounding the role of black carbon in the climate system: A Scientific assessment, J. Geophys. Res.-Atmos., 118, 5380–5552, doi:10.1002/jgrd.50171, 2013.

Clarke, A.D., and Noone, K.J.: Soot in the Arctic snowpack: a cause for perturbations in radiative transfer, Atmos. Environ., 19, 2045-2053, doi: 10.1016/0004-6981(85)90113-1, 1985.

Fibiger, D. L., Dibb, J. E., Chen, D., Thomas, J. L., Burkhart, J. F., Huey, L. G., and Hastings, M. G.: Analysis of nitrate in the snow and atmosphere at Summit, Greenland: Chemistry and transport, J. Geophys. Res.-Atmos., 121, 5010–5030, doi:10.1002/2014JD022297, 2016.

Flanner, M. G., Zender, C. S., Randerson, J. T., and Rasch, P. J.: Present-day climate forcing and response from black carbon in snow, J. Geophys. Res.-Atmos., 112 (September 2006), 1–17, doi:10.1029/2006JD008003, 2007.

Freedman, B., Zobens, V., Hutchinson, T. C., and Gizyn, W. I.: Intense, natural pollution affects Arctic tundra vegetation at the Smoking Hills, Canada, Ecology, 71 (2), 492–503, doi:10.2307/1940303, 1990.

Hansen, J. and Nazarenko, L.: Soot climate forcing via snow and ice albedos, P. Natl. Acad. Sci. USA, 101 (2), 423–428, doi:10.1073/pnas.2237157100, 2004.

Hartmann, D. J., Klein Tank, A. M. G., Rusticucci, M., Alexander, L. V., Brönnimann, S., Charabi, Y. A.-R., Dentener, F. J., et al.: Observations: Atmosphere and surface, Climate change 2013: The Physical science basis, Contribution of working group I to the fifth assessment report of the Intergovernmental Panel on Climate Change [Stocker, T.F., D. Qin, G.-K. Plattner, M. Tignor, S.K. Allen, J. Boschung, A. Nauels, Y. Xia, V. Bex and P.M. Midgley (eds.)], Cambridge University Press, Cambridge and New York, NY, doi:10.1017/CBO9781107415324.008, 2013.

Hays, M. D., Fine, P. M., Geron, C. D., Kleeman, M. J., and Gullett, B. K.: Open burning of agricultural biomass: Physical and chemical properties of particle-phase emissions, Atmos. Environ., 39 (36), 6747–6764, doi:10.1016/j.atmosenv.2005.07.072, 2005.

Hegg, D. A., Warren, S. G., Grenfell, T. C., Doherty, S. J., Larson, T. V., and Clarke, A. D.: Source attribution of black carbon in Arctic snow, Environ. Sci. Techno., 43 (11), 4016–4021, doi:10.1021/es803623f, 2009.

Hegg, D. A., Warren, S. G., Grenfell, T. C., Doherty, S. J., and Clarke, A. D.: Sources of light-absorbing aerosol in Arctic snow and their seasonal variation, Atmos. Chem. Phys., 10, 10923–10938, doi:10.5194/acp-10-10923-2010, 2010.

Henry, R. C., Lewis, C. W., Hopke, P. K., and Williamson, H. J.: Review of receptor model fundamentals, Atmos. Environ. (1967), 18 (8), 1507–1515, doi:10.1016/0004-6981(84)90375-5, 1984.

Hopke, P. K., Barrie, L. A., Li, S.-M., Cheng, M.-D., Li, C., and Xie, Y.: Possible sources and preferred pathways for biogenic and non-sea-salt sulfur for the high Arctic, J. Geophys. Res., 100 (95), 16595, doi:10.1029/95JD01712, 1995.

Huang, K., Fu, J. S., Prikhodko, V. Y., Storey, J. M., Romanov, A., Hodson, E. L., Cresko, J., Morozova, I., Ignatieva, Y., and Cabaniss, J.: Russian anthropogenic black carbon: Emission reconstruction and Arctic black carbon simulation, J. Geophys. Res.-Atmos., 120 (21), 11306–11333, doi:10.1002/2015JD023358, 2015.

Jaffrezo, J.-L., Davidson, C. I., Kuhns, H. D., Bergin, M. H., Hillamo, R., Maenhaut, W., Kahl, J. W., and Harris, J. M.: Biomass burning signatures in the atmosphere of central Greenland, J. Geophys. Res., 103, (D23), 31067-3108, doi:10.1029/98JD02241, 1998.

Jiao, C., Flanner, M. G., Balkanski, Y., Bauer, S. E., Bellouin, N., Berntsen, T. K., Bian, H., et al.: An Aerocom assessment of black carbon in Arctic snow and sea ice, Atmos. Chem. Phys., 14 (phase I), 2399–2417, doi:10.5194/acp-14-2399-2014, 2014.

Laing, J. R., Hopke, P. K., Hopke, E. F., Husain, L., Dutkiewicz, V. A., Paatero, J. and Viisanen, Y.: Long-term particle measurements in Finnish Arctic: Part II - Trend analysis and source location identification, Atmos. Environ., 88, Elsevier Ltd, 285–296, doi:10.1016/j.atmosenv.2014.01.015, 2014.

Law, K. S. and Stohl, A.: Arctic air pollution: Origins and impacts, Science, 315, 1537–1540, doi:10.1126/science.1137695, 2007.

Legrand, M., and de Angelis, M.: Origins and variations of light carboxylic acids in polar precipitation, J. Geophys. Res., 100 (Di), 1445–1462, doi:10.1029/94jd02614, 1995.

Legrand, M., and De Angelis, M.: Light carboxylic acids in Greenland ice: A Record of past forest fires and vegetation emissions from the boreal zone, J. Geophys. Res., 101 (D2), 4129-4145, doi:10.1029/95JD03296, 1996.

Li, S. M., Barrie, L. A., Talbot, R. W., Harriss, R. C., Davidson, C. I., and Jaffrezo, J. L.: Seasonal and geographic variations of methanesulfonic acid in the Arctic troposphere, Atmos. Environ. A-Gen., 27 (17-18), 3011–3024, doi:10.1016/0960-1686(93)90333-T, 1993.

Macdonald, K. M., Sharma, S., Toom, D., Chivulescu, A., Hanna, S., Bertram, A. K., Platt, A., Elsasser, M., Huang, L., Tarasick, D., Chellman, N., McConnel, J., Bozem, H., Kunkel, D., Ying Duan, L., Evans, G. J., and Abbatt, J. P. D.: Observations of atmospheric chemical deposition to high Arctic snow, Atmos. Chem. Phys., doi:10.5194/acp-17-5775-2017, 2017.

Masson-Delmotte, V., Schulz, M., Abe-Ouchi, A., Beer, J., Ganopolski, A., Rouco, J. F. G., Jansen, E., et al.: Information from paleoclimate archives, Climate change 2013: The Physical science basis, Contribution of working group I to the fifth assessment report of the Intergovernmental Panel on Climate Change, 383–464, doi:10.1017/CBO9781107415324.013, 2013.

McMeeking, G. R., Kreidenweis, S. M., Baker, S., Carrico, C. M., Chow, J. C., Collett, J. L., Hao, W. M., et al.: Emissions of trace gases and aerosols during the open combustion of biomass in the laboratory, J. Geophys. Res.-Atmos., 114 (19), 1–20, doi:10.1029/2009JD011836, 2009.

Morin, S., Savarino, J., Frey, M. M., Yan, N., Bekki, S., Bottenheim, J. W., and Martins, J. M. F.: Tracing the origin and fate of NOx in the Arctic atmosphere using stable isotopes in nitrate, Science, 322, 730–732, doi:10.1126/science.1161910, 2008.

Mungall, E. L., Abbatt, J P. D., Wentzell, J. J. B., Lee, A. K. Y., Thomas, J. L., Blais, M., Gosselin, M., Miller, L. A., Papakyriakou, T., Willis, M. D., and Liggio, J.: Microlayer source of oxygenated volatile organic compounds in the summertime marine Arctic boundary layer, Proceedings of the National Academy of Sciences, 114 (24), 6203–6208, doi: 10.1073/pnas.1620571114, 2017.

Nguyen, Q. T., Skov, H., Sørensen, L. L., Jensen, B. J., Grube, A. G., Massling, A., Glasius, M., and Nøjgaard, J. K.: Source apportionment of particles at Station Nord, north east Greenland during 2008-2010 using COPREM and PMF analysis, Atmos. Chem. Phys., 13, 35–49, doi:10.5194/acp-13-35-2013, 2013.

Norris, G., Duvall, R., Brown, S., and Bai. S.: EPA Positive matrix factorization (PMF) 5.0 fundamentals and user guide, U.S. Environmental Protection Agency, 2014.

Paatero, P. and Hopke. P. K.: Discarding or downweighting high-noise variables in factor analytic models, Anal. Chim. Acta, 490, 277–289, doi:10.1016/S0003-2670(02)01643-4, 2003.

Paatero, P., Eberly, S., Brown, S. G., and Norris, G. A.: Methods for estimating uncertainty in factor analytic solutions, Atmospheric Measurement Techniques, 7 (2008), 781–797, doi:10.5194/amt-7-781-2014, 2014.

Paris, J.-D., Stohl, A., Nédélec, P., Arshinov, M. Y., Panchenko, M. V., Shmargunov, V. P., Law, K. S., Belan, B. D., and Ciais, P.: Wildfire smoke in the Siberian Arctic in summer: Source characterization and plume evolution from airborne measurements, Atmos. Chem. Phys. Discussions, 9, 18201–18233, doi:10.5194/acpd-9-18201-2009, 2009.

Paulot, F., Wunch, D., Crounse, J. D., Toon, G. C., Millet, D. B., DeCarlo, P. F., Vigouroux, C., Deutscher, N. M., González Abad, G., Notholt, J., Warneke, T., Hannigan, J. W., Warneke, C., de Gouw, J. A., Dunlea, E. J., De Mazière, M., Griffith, D. W. T., Bernath, P., Jimenez, J. L., and Wennberg, P. O.: Importance of secondary sources in the atmospheric budgets of formic and acetic acids, Atmos. Chem. Phys., 11, 1989-2013, doi10.5194/acp-11-1989-2011, 2011.

Pytkowicz, R. M. and Kester, D. R.: The Physical chemistry of sea water, Oceanogr. Mar. Biol., 9, 11–60, doi:10.1029/WR001i002p00263, 1971.

Quinn, P. K., Shaw, G., Andrews, E., Dutton, E. G., Ruoho-Airola, T., and Gong, S. L.: Arctic haze – Current trends and knowledge gaps, Tellus B., 59 (1), 99–114, doi:10.1111/j.1600-0889.2006.00238.x, 2007.

Reff, A., Eberly, S. I., and Bhave, P. V.: Receptor modeling of ambient particulate matter data using positive matrix factorization: Review of existing methods, Journal of the Air and Waste Management Association (1995), 57 (August 2014), 146–154, doi:10.1080/10473289.2007.10465319, 2007.

Saarikoski, S., Sillanpaa, M., Sofiev, M., Timonen, H., Saarnio, K., Teinila, K., Karppinen, A., Kukkonen, J., and Hillamo, R.: Chemical composition of aerosols during a major biomass burning episode over northern Europe in spring 2006: Experimental and modelling assessments, Atmos. Environ., 41 (17), 3577–3589, doi:10.1016/j.atmosenv.2006.12.053, 2007.

Sirois, A. and Barrie, L. A.: Arctic lower tropospheric aerosol trends and composition at Alert, Canada: 1980–1995, J. Geophys. Res., 104 (D9), 11599–11618, doi:10.1029/1999JD900077, 1999.

Skeie, R. B., Berntsen, T., Myhre, G., Pedersen, C. A., Strãm, J., Gerland, S., and Ogren, J. A.: Black carbon in the atmosphere and snow, from pre-industrial times until present, Atmos. Chem. Phys., 11, 6809–6836, doi:10.5194/acp-11-6809-2011, 2011.

Slater, J. F., Currie, L. A., Dibb, J. E., and Benner, B. A.: Distinguishing the relative contribution of fossil fuel and biomass combustion aerosols deposited at Summit, Greenland through isotopic and molecular characterization of insoluble carbon, Atmos. Environ., 36 (28), 4463–4477, doi:10.1016/S1352-2310(02)00402-8, 2002.

Stohl, A., Forster, C., Frank, A., Seibert, P., and Wotawa, G.: Technical note – The Lagrangian particle dispersion model FLEXPART version 6.2, Atmos. Chem. Phys., 5(9), 2461–2474, doi:10.5194/acp-5-2461-2005, 2005.

Stohl, A.: Characteristics of atmospheric transport into the Arctic troposphere, J. Geophys. Res.-Atmos., 111 (February), 1–17, doi:10.1029/2005JD006888, 2006.

Stohl, A., Klimont, Z., Eckhardt, S., Kupiainen, K., Shevchenko, V. P., Kopeikin, V. M., and Novigatsky, A. N.: Black carbon in the Arctic: The Underestimated role of gas flaring and residential combustion emissions, Atmos. Chem. Phys., 13, 8833–8855, doi:10.5194/acp-13-8833-2013, 2013.

Taylor, S. R.: Abundance of chemical elements in the continental crust: A New table, Geochim. Cosmochim. Ac., 28 (8), 1273–1285, doi:10.1016/0016-7037(64)90129-2, 1964.

Turn, S. Q., Jenkins, B. M., Chow, J. C., Pritchett, L. C., Campbell, D., Cahill, T., and Whalen, S. A.: Elemental characterization of particulate matter emitted from biomass burning: Wind tunnel derived source profiles for herbaceous and wood fuels, J. Geophys. Res.-Atmos., 102 (D3), 3683–3699, doi:10.1029/96JD02979, 1997.

Wang, Q., Jacob, D. J., Fisher, J. A., Mao, J., Leibensperger, E. M., Carouge, C. C., Le Sager, P., et al.: Sources of carbonaceous aerosols and deposited black carbon in the Arctic in winter-spring: Implications for radiative forcing, Atmos. Chem. Phys., 11, 12453–12473, doi:10.5194/acp-11-12453-2011, 2011.

Xu, J., Martin, R. V., Morrow, A., Sharma, S., Huang, L., Leaitch, W. R., Burkart, J., Schulz, H., Zanatta, M., Willis, M. D>., Henze, D. K., Lee, C. J., Herber, A. B., and Abbatt, J. P. D.: Source attribution of Arctic black carbon constrained by aircraft and surface measurements, Atmos. Chem. Phys. Discuss., https://doi.org/10.5194/acp-2017-236, in review, 2017.

Xu, L., Russell, L. M., Somerville, R. C. J., and Quinn, P. K.: Frost flower aerosol effects on arctic wintertime longwave cloud radiative forcing, J. Geophys. Res.-Atmos., 118 (23), 13282–13291, doi:10.1002/2013JD020554, 2013.

Ye, P., Xie, Z., Yu, J., and Kang, H.: Spatial distribution of methanesulphonic acid in the Arctic aerosol collected during the Chinese Arctic research expedition, Atmos., 6 (5), 699–712, doi:10.3390/atmos6050699, 2015.

Yttri, K. E., Simpson, D., Nojgaard, J. K., Kristensen, K., Genberg, J., Stenström, K., Swietlicki, E., et al.: Source apportionment of the summer time carbonaceous aerosol at Nordic rural background sites, Atmos. Chem. Phys., 11 (24), 13339–13357, doi:10.5194/acp-11-13339-2011, 2011.

Yttri, K. E., Myhre, C. L., Eckhardt, S., Fiebig, M., Dye, C., Hirdman, D., Ström, J., Klimont, Z., and Stohl, A.: Quantifying black carbon from biomass burning by means of levoglucosan - A One-year time series at the Arctic observatory Zeppelin, Atmos. Chem. Phys., 14, 6427–6442, doi:10.5194/acp-14-6427-2014, 2014.

Zwaaftink,C. D. G., Grythe, H., Skov, H., and Stohl, A.: Substantial contribution of northern high-latitude sources to mineral dust in the Arctic, J. Geophys. Res.-Atmos., 121, 13,678–13,697, doi:10.1002/2016JD025482, 2016.